Low Temperature NH($X\ ^3\Sigma^-$) Radical Reactions with NO, Saturated, and Unsaturated Hydrocarbons Studied in a Pulsed Supersonic Laval Nozzle Flow Reactor between 53 and 188 K

Christopher Mullen and Mark A. Smith*

Department of Chemistry, University of Arizona, 1306 East University Drive, Tucson, Arizona 85721

Received: September 30, 2004; In Final Form: December 8, 2004

The reactions of ground-state imidogen radicals (NH($X\ ^3\Sigma^-$)) with NO and select saturated and unsaturated hydrocarbons have been measured in a pulsed supersonic expansion Laval nozzle flow reactor in the temperature range 53−188 K. The rate coefficients for the NH + NO system display negative temperature dependence in the temperature regime currently investigated and a global temperature-dependent fit is best represented in a modified power law functional form, with $k_1(\mathrm{NH} + \mathrm{NO}) = (4.11 \pm 0.31) \times 10^{-11} \times (T/300)^{(-0.30\pm0.17)} \times \exp^{(77\pm21/T)}$ cm^3/s. The reactions of NH with ethylene, acetylene, propene, and diacetylene were measured over the temperature range 53−135 K. In addition, the reactions of NH with methane and ethane were also measured at 53 K, for reasons discussed later. The temperature dependence of the reactions of NH with the unsaturated hydrocarbons are fit using power law expressions, $k(T) = A(T/300)^{-n}$, and are as follows: $k_4 = (2.3 \pm 1.2) \times 10^{-12} \times (T/300)^{(-1.09\pm0.33)}$ cm^3/s, $k_5 = (4.5 \pm 0.3) \times 10^{-12} \times (T/300)^{(-1.07\pm0.04)}$ cm^3/s, $k_6 = (5.6 \pm 1.9) \times 10^{-12} \times (T/300)^{(-1.23\pm0.21)}$ cm^3/s, and $k_7 = (7.4 \pm 1.8) \times 10^{-12} \times (T/300)^{(-1.23\pm0.15)}$ cm^3/s for ethylene, acetylene, propene, and diacetylene, respectively. The rate for NH + ethane at 53 K is measured to be $k_3 = (6.8 \pm 1.7) \times 10^{-12}$ cm^3/s, while that for methane at the same temperature represents an upper bound of $k_2 \leq (1.1 \pm 4.3) \times 10^{-12}$ cm^3/s, as this is at the limits of measurement with our current technique. The behavior of these systems throughout the temperature range explored indicates that these reactions occur over a potential energy surface without an appreciable barrier through a complex formation mechanism. Implications for chemistry in low temperature environments where these species are found are briefly discussed.

1. Introduction

The ground-state NH($X\ ^3\Sigma^-$) radical is a chemically interesting species capable of participating in a rich set of chemistries mechanistically ranging from insertion to abstraction to addition. Studies of NH reactions with a variety of partners have been conducted from room temperature up to temperatures relevant to combustion processes. In particular, studies of NH with NO have been investigated at high temperatures in shock heated gases,[1,2] in flames,[3,4] and at room temperature and above in order to gain experimental information on the mechanism and branching ratio of a relatively simple reactive system.[5−9] In addition, high-temperature studies of NH with hydrocarbons have been conducted to investigate the role of abstraction and addition pathways.[10−12] The self-reaction[13] and those of NH + OH[14] and NH + O_2,[1,14−17] have also been reported, and to the best of our knowledge, no studies below 250 K with any partner have been conducted.

NH radical has been detected in the atmosphere of Titan. This species is thought to be formed by reaction of N(^{2}D) with H_2, but is not included in global rate models except with methyl, vinyl, and ethyl radicals.[18] Experimental investigations of N(^{2}D) + H_2 find this to be a viable formation pathway.[19,20] Also explored are the dynamics of the reaction of N(^{2}D) atoms with acetylene. The primary reaction product is found to be cyanomethylene (HCCN), and reactions of this type are implicated in the formation of nitriles in the upper atmosphere of Titan.[21] Reactions of the CN radical with hydrocarbons found in the atmosphere of Titan are also included in the chemical network, the products of which are also nitriles. Low-temperature rate measurements have verified the feasibility of these addition/elimination routes for acetylene, ethylene,[22] allene, and methyl acetylene,[23] as well as an abstraction pathway for CN with ethane.[22] NH addition chemistry, although not currently considered in the modeling of planetary atmospheres, is of importance as the products of these reactions will similarly lead to the incorporation of nitrogen into carbon containing molecules. Their lack of inclusion in chemical models is probably due to their slow rate of reaction at room temperature and above. However, a variety of neutral−neutral systems are now found that exhibit non-Arrhenius behavior at low temperature[24] due to the effects of long-range electrostatic interactions, increased collision complex lifetimes, and reaction surfaces without a potential barrier. Manifestation of these conditions results in appreciable reaction rates as the temperature is decreased, thus requiring accurate rate data measurements in the temperature regime of interest for the chemical modeling of planetary atmospheres and interstellar environments such as dense molecular clouds.

In the present paper we apply the pulsed Laval expansion supersonic flow technique to the study of NH radical reactions at low temperature and elucidate their behavior in a temperature regime important to the interstellar medium and planetary

* Corresponding author. E-mail: msmith@u.arizona.edu.

10.1021/jp045541f CCC: $30.25
Published on Web 02/01/2005

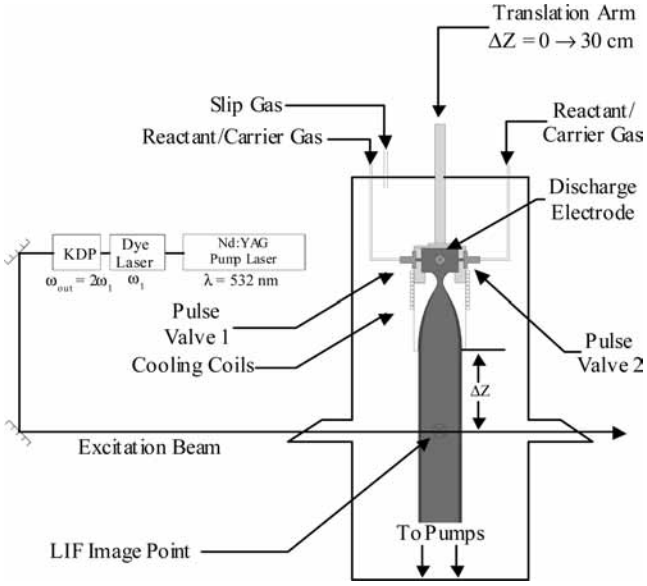

Figure 1. Schematic diagram of the pulsed supersonic Laval nozzle flow reactor.

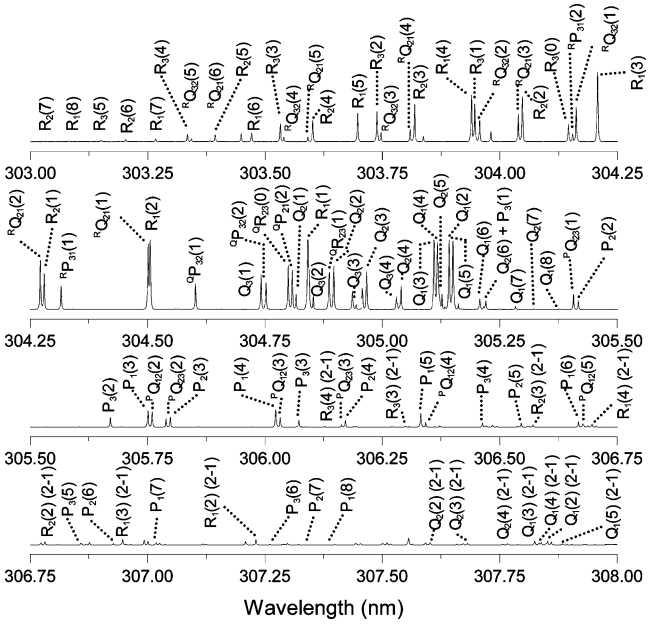

Figure 2. Laser induced fluorescence spectrum of NH ($X^3\Sigma^- \rightarrow A\ ^3\Pi$, $v'' = 0 \rightarrow v' = 1$) radical in a 190 K nitrogen Laval flow.

atmospheres such as Titan. The rate coefficients for the following reactions have been measured between 53 and 188 K:

$$NH + NO \xrightarrow{k_1} \text{products} \quad \text{(R1)}$$

$$NH + CH_4 \xrightarrow{k_2} \text{products} \quad \text{(R2)}$$

$$NH + C_2H_6 \xrightarrow{k_3} \text{products} \quad \text{(R3)}$$

$$NH + C_2H_4 \xrightarrow{k_4} \text{products} \quad \text{(R4)}$$

$$NH + C_2H_2 \xrightarrow{k_5} \text{products} \quad \text{(R5)}$$

$$NH + C_3H_6 \xrightarrow{k_6} \text{products} \quad \text{(R6)}$$

$$NH + C_4H_2 \xrightarrow{k_7} \text{products} \quad \text{(R7)}$$

Reaction R1 was chosen as a prototype reaction with which to calibrate the performance of our flow technique, as kinetic data at slightly higher temperature is available.[6] The reactants in (R2) through (R7) were chosen as they are important constituents in the atmosphere of Titan, and their low temperature chemistry with NH was previously unexplored. Reaction R2 served as a further calibrant for the technique as the heat of reaction for the H atom abstraction process is positive, and thus, the reaction should not be appreciably active at the temperatures employed. The heat of formation of the NH($X\ ^3\Sigma^-$) radical leaves some uncertainty in the heat of reaction for reaction R3, while all others, (R4) through (R7), should possess exothermic product channels.

2. Experimental Section

A detailed description of our pulsed uniform supersonic expansion flow reactor is presented elsewhere, and thus only a pertinent overview will be given here.[25,26] A schematic diagram of the instrument is shown in Figure 1.

The kinetics of reactions R1−R7 are studied by co-expanding known quantities of reagent and buffer gases through a supersonic pulsed Laval nozzle. The Laval nozzle creates a unique low-temperature environment in which the post nozzle flow is in local thermodynamic equilibrium, with a well-defined hydrodynamic velocity and density. These conditions can be maintained for a number of centimeters past the exit (ΔZ of Figure 1), typically 20, providing a few hundred microsecond window in which reaction kinetics can be monitored. All kinetic studies were conducted under pseudo first-order conditions in which the concentration of the reactant, i.e., [NO] or [hydrocarbon], was in excess of the NH radical. NH radicals are created using a pulsed dc discharge in the stagnation volume, from a mixture of less than 1% H_2 in N_2, for the nitrogen nozzles employed, or a mixture of a few percent H_2 and N_2 in Ar, for the 53 K measurements employing an argon buffer. Time dependent evolution of NH radical density was monitored using laser-induced fluorescence (LIF). The NH radical $X\ ^3\Sigma^- \rightarrow A\ ^3\Pi$ ($v'' = 0 \rightarrow v' = 1$) transition was excited using a tunable dye laser (Continuum model ND60) operating with Rhodamine 640 dye, which was pumped by a 10 Hz pulsed Nd:YAG laser (Continuum model NY61).The primary dye radiation was doubled in a KD*P crystal producing tunable light near 305 nm. Laser frequency calibration was accomplished using the optogalvanic lines of Fe and Ne pumped with the dye laser fundamental. In all cases the $R_{P31}(1)$ transition at $\sim$ 304.32 nm was used for kinetic studies. A 188 K spectrum of the $X \rightarrow A$ ($v'' = 0 \rightarrow v' = 1$) band taken in the N2M21e17 nozzle, is shown in Figure 2. The transitions are labeled in J''. Spectral assignment was accomplished based on previous work.[27−29]

The resulting ($1 \rightarrow 1$) fluorescence was collected with a photomultiplier tube (Hamamatsu R3896) situated perpendicular to the flow axis employing an appropriate filter set (Schott glass BG-40 and Corning 7-60). This band was chosen to minimize scattered light in the collection system and also to maximize signal, based on the Franck−Condon factors between the two states.[30] The LIF signal was amplified and sent to either a boxcar integrator (SRS 250) or an oscilloscope (LeCroy 9400) and averaged for 200 to 500 shots. The gases used for these studies are as follows: methane, Matheson C.P., 99%, propene, Matheson, Research 99.97%, ethane, Matheson, C.P., 99%, ethylene, Matheson, Research, 99.999%, acetylene, Matheson, Purified, 99.6%, H_2, AirLiquide, 99.95%, N_2, US Airweld,

99.99%, and Ar, US Airweld, UHP, 99.999%. Diacetylene was prepared by the dehydrohalogenation of 1,4-dichloro-2-butyne[31] in DMSO, by gentle heating of the mixture to 75 °C, with dropwise addition of a 20% w/w solution of NaOH over the course of 30 min. The diacetylene generated from the reaction was dried in a calcium chloride/P_2O_5 trap, and then immediately condensed in a liquid N_2 trap, for storage. This sample was then transferred to a mixing tank and diluted to less than 1% in N_2 and used as such. The purity of the sample was checked via IR absorption and was found to be in excess of 99%.

Essential to the successful execution of these measurements is precise knowledge of the post nozzle flow conditions where the chemical reaction studies take place. In particular, one is interested in the distance for which flow uniformity, in both density and temperature, is maintained. The final supersonic flow parameters are linked to the preexpansion conditions through the Mach number of the flow and the isentropic relationship, eqs 1 and 2

$$\frac{T}{T_0} = \left(1 + \frac{\gamma - 1}{2} M^2\right)^{-1} \quad (1)$$

$$\frac{\rho}{\rho_0} = \left(1 + \frac{\gamma - 1}{2} M^2\right)^{-1/\gamma - 1} \quad (2)$$

where M is the Mach number, ρ_0 is the stagnation density, and γ is the heat capacity ratio C_p/C_v. The flow uniformity is verified using an impact pressure transducer, or Pitot probe, placed in the path of the flow, approximately 3 cm below the laser probe beam. The measured impact pressures, P_i, can be converted into a Mach number using the Rayleigh−Pitot formula (eq 3)

$$\frac{P_i}{P_s} = \left(\frac{\gamma + 1}{2} M^2\right)^{\gamma/\gamma - 1} \left(\frac{\gamma + 1}{2\gamma M^2 - (\gamma - 1)}\right)^{1/\gamma - 1} \quad (3)$$

where P_s is the static flow pressure, and the other symbols are the same as defined for the isentropic relationship. The flow Mach number is then used in conjunction with the isentropic expansion relationship, eq 1, and knowledge of T_0 to extract the flow temperature. In addition, the flow temperature can also be probed using laser-induced fluorescence, by scanning a number of rotational branch transitions and relating the individual fluorescence intensities to the population in that rotational state through the rotational line strengths and the Boltzmann equation. Line intensities were obtained by integrating the individual line profiles. Both methods, pitot and LIF, are found to agree within their respective errors, for all nozzles used in this study. Flow conditions for the N2M33e16 nozzle are depicted in Figure 3. A summary of the flow conditions for the nozzles characterized and used in these studies can be viewed in Table 1. The LIF temperatures reported in Table 1 were

TABLE 1: Calibrated Nozzle Flow Characteristics. T_{Flow}(LIF) is Derived from the Rotational Temperature from Laser Induced Fluorescence Experiments on Either the OH or OD Radical. T_{Flow}(Impact) is from Pitot Measurements

nozzle	Mach no.[a]	stagnation temp (K)	T_{Flow}(LIF) (K)	T_{Flow}(Impact) (K)	flow density (10^{16} cm^{-3})
ArM32e16	3.5	263	53 ± 4	53 ± 3	3.2 ± 0.2
N2M32e16	3.2	273	83 ± 3	89 ± 5	1.7 ± 0.2
N2M33e16	2.5	300	135 ± 11	132 ± 6	4.5 ± 0.5
N2M21e17	1.7	300	188 ± 7	183 ± 4	14.1 ± 0.6

[a] Mach number derived from LIF temperatures.

derived from separate experiments using the X $^2\Pi_{3/2} \rightarrow$ A $^2\Sigma$ ($v'' = 0 \rightarrow v' = 1$) S_{21} branch transitions of either the OH or

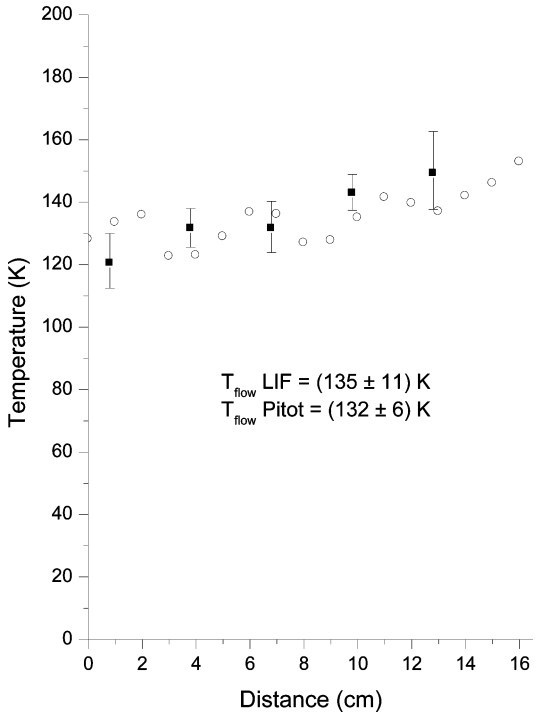

Figure 3. Characterization of the N2M33e16 nozzle exit temperature via impact and LIF measurements. ○ − Impact pitot measurement, ■ − LIF measurement with OD radical.

OD radical. In addition, it was desirable to verify that the NH radical rotational population was equilibrated in the flows, under conditions used for the kinetic experiments. Therefore, the R_1, R_2, R_3, P_1, P_2, and P_3 branch transitions from Figure 2 were subjected to analysis and yield a flow temperature ($T = 176 \pm 10$ K) that agrees within experimental error to the temperature derived from OH LIF measurements ($T = 188 \pm 7$ K) and pitot impact measurements ($T = 183 \pm 4$ K) for the N2M21e17 nozzle. Figure 4 shows the Boltzmann plot used to obtain the temperature. The rotational line strength factors, S_{ij}, and rotational term energies were taken from Lucht et al.[32] The agreement for the other nozzles, as regards NH equilibration, is assumed.

3. Results

Rate coefficients for the reactions of imidogen radical with NO and the hydrocarbons were measured under pseudo first-order conditions, such that the concentration of the reactant was much larger than that of the NH concentration. Under these conditions the loss rate of NH can be expressed as

$$\frac{d[NH]}{dt} = -k[NH][R] = -k'[NH] \quad \text{with } k' = k[R] \quad (4)$$

where [NH] and [R] represent the concentration of the imidogen radical and reactant in the final supersonic flow, respectively. Rearrangement and integration of eq 4, with the assumption that $d[R]/dt = 0$, yields

$$\ln\left(\frac{NH_{(Z)}}{NH_{(Z_0)}}\right) = \frac{k'}{u}(Z - Z_0) \quad (5)$$

Since the hydrodynamic flow velocity u is well-defined and $du/dt = 0$ in the post nozzle Laval flow region, the reaction

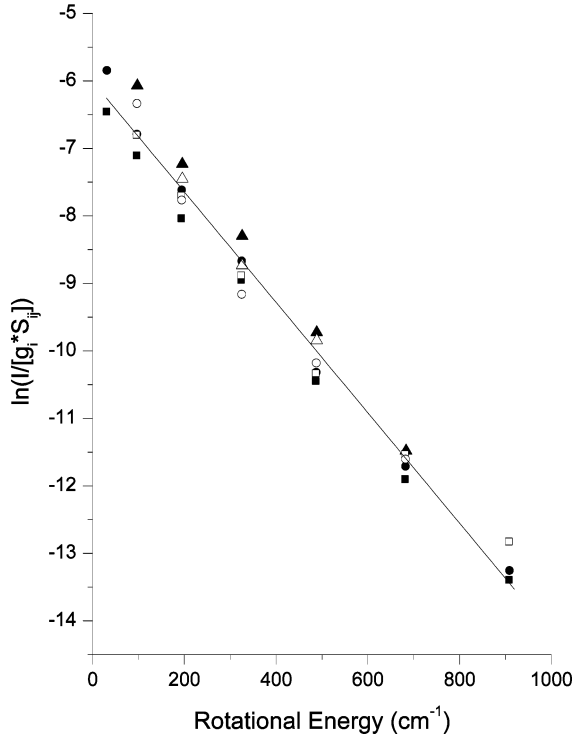

Figure 4. Boltzmann plot of the R and P branch transitions of the NH X→ A ($v'' = 0 \rightarrow v' = 1$) transition used to extract the flow temperature. ■ − R_1, ● − R_2, ▲ − R_3, □ − P_1, ○ − P_2, △ − P_3.

time t can be obtained from the relationship $\Delta t = \Delta Z/u$, where ΔZ is the distance between the nozzle exit and the laser probe. The second order rate coefficient k, is extracted by monitoring the distance dependent decay of NH via the LIF method at 8−10 different positions in the flow, in the presence of a known concentration of R. This measurement was then repeated for between 5 and 10 different concentrations of R, while holding the rest of the experimental parameters constant. Flow conditions were constantly monitored throughout the duration of the kinetic runs, using both the stagnation and impact transducers, to ensure uniformity. Plots of the natural logarithm of the normalized signal vs distance, yield the pseudo first-order decay constant k', Figure 5a. Linear least-squares fitting is used to extract k'. The individual k' values are then plotted against the concentration of reactant R, under which they were obtained, Figure 5b. The slope equals the second order rate coefficient and is extracted in a similar fashion, using linear least-squares fitting. The linearity of both plots validates pseudo first order conditions. The nonzero intercept in Figure 5b, at [R] = 0, is most likely due to reactivity of NH with other species in the flow, and possibly to some extent diffusional loss, but in all cases represents only a small portion of the total NH decay in the presence of reactant.

The temperature-dependent rate coefficients determined from these studies, for the reaction partners nitric oxide, methane, ethane, ethylene, acetylene, propene, and diacetylene are summarized in Table 2. The inverse temperature dependence of the rate of reaction of NH with NO is illustrated in Figure 6, along with previous experimental measurements made by Harrison et al. in the 250−400K window, using a Pyrex photolysis cell.[6] The best fit to the entire data set is found to be $k(T) = (4.11 \pm 0.31) \times 10^{-11} \times (T/300)^{(0.30\pm0.17)} \times \exp^{((77\pm21)/T)}$ cm^3 s^{-1}.

Figure 7 depicts the temperature dependence for the reactions of NH with the unsaturated hydrocarbons ethylene, acetylene, propene, and diacetylene between 53 −135 K, along with single

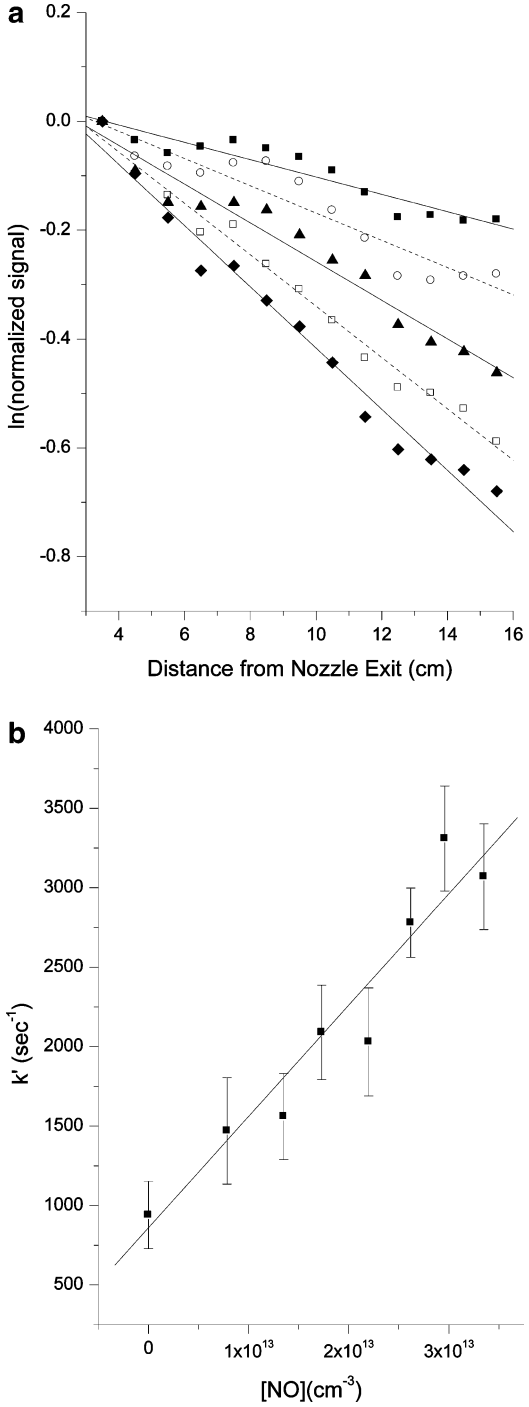

Figure 5. (a) Pseudo 1st order decays for NH + NO in the N2M32e16 nozzle. Percent NO in flow: ■ − 0.00, ○ − 0.05, ▲ − 0.10, □ − 0.15, ◆ − 0.17. (b) Plot of k' vs [NO] used to extract the bimolecular rate coefficient.

temperature measurements for methane and ethane at 53 K. Best fits to the power law functional form; $A(T/300)^{-n}$, are given in Table 3. Figure 8 includes the data from the studies of Rohrig et al. at temperatures above 1000 K, conducted in incident shock waves in an aluminum shock tube apparatus.[11,12]

4. Discussion

4a. NH + NO. Studies on the NH + NO reaction system were initially conducted for a number of reasons. Past work on this system indicated that the reactivity was fairly constant over the temperature range investigated and that the reaction pro-

TABLE 2: Rate Coefficients for the Reactions of NH Radical with NO, Saturated, and Unsaturated Hydrocarbons

reactant	nozzle	temp (K)	[R] (10^{13} cm^{-3})[a]	k(10^{-11} cm^3 molecule^{-1} s^{-1})
NO	ArM32e16	53	1.3	10.46 ± 0.89
methane	ArM32e16	53	1.9	0.105 ± 0.432
ethane	ArM32e16	53	4	0.68 ± 0.165
ethylene	ArM32e16	53	3.9	1.55 ± 0.16
acetylene	ArM32e16	53	1.6	2.88 ± 0.49
propene	ArM32e16	53	1.6	4.64 ± 0.7
diacetylene	ArM32e16	53	1.1	6.34 ± 0.75
NO	N2M32e16	83	2.4	7.11 ± 0.35
ethylene	N2M32e16	83	3.2	0.786 ± 0.189
acetylene	N2M32e16	83	1.9	1.82 ± 0.69
propene	N2M32e16	83	1.6	2.97 ± 0.77
diacetylene	N2M32e16	83	1	3.37 ± 0.65
NO	N2M33e16	135	2.4	5.92 ± 1.17
ethylene	N2M33e16	135	5.5	0.658 ± 0.123
acetylene	N2M33e16	135	4.5	1.03 ± 0.5
propene	N2M33e16	135	2.1	1.28 ± 0.28
diacetylene	N2M33e16	135	1.9	2.19 ± 0.32
NO	N2M21e17	188	8.9	5.63 ± 1.57

[a] [R] represents the maximum concentration of reactant used to obtain the bimolecular rate coefficient.

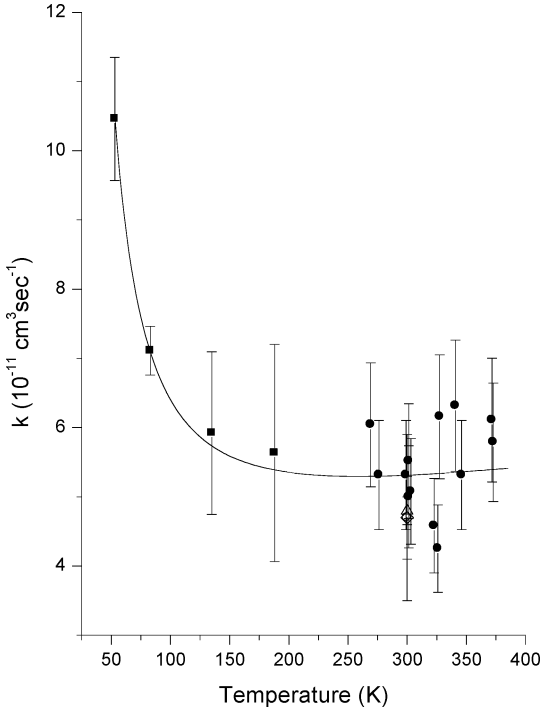

Figure 6. The temperature dependence of the reaction rate coefficient for NH ($X^3\Sigma^-$) + NO: ■ − this work, ● − Harrison et al.,[6] △ − Cox et al.,[8] ○ − Hansen et al.,[7] ◇ − Yamasaki et al.[9] The line represents the best fit over the temperature range of 53−375 K to the functional form $k(T) = A \times (T/300)^n \times \exp^{(-b/T)}$.

TABLE 3: Best Fit Parameters to the $k(T) = A \times (T/300)^{-n}$ Power Law Functional Form for the Unsaturated Hydrocarbons Studied

reactant	A (10^{-12} cm^3 s^{-1})	$-n$
ethylene	2.3 ± 1.2	1.09 ± 0.33
acetylene	4.5 ± 0.3	1.07 ± 0.04
propene	5.6 ± 1.9	1.23 ± 0.21
diacetylene	7.4 ± 1.8	1.23 ± 0.15

ceeded through a complex formation mechanism involving the HNNO species.[6−8] Rates weakly dependent on temperature in a region near room temperature and above are generally indicative of a reaction occurring over an attractive potential

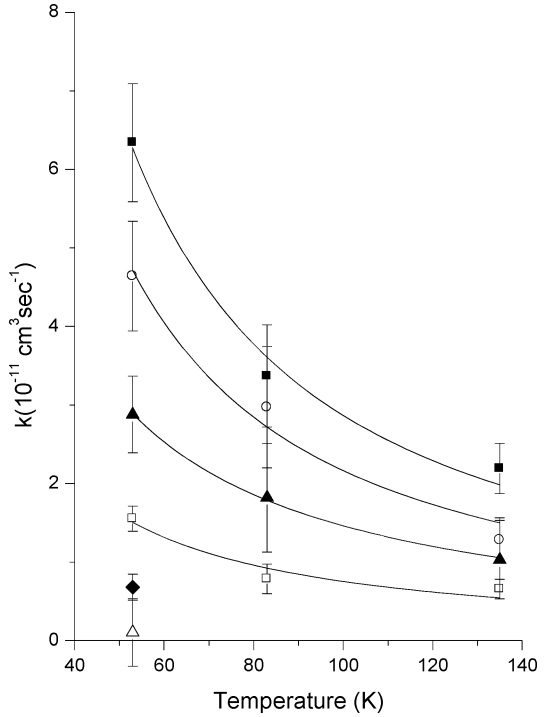

Figure 7. Temperature dependent rate coefficients for the reactions of NH ($X^3\Sigma^-$) with: ■ − diacetylene, ○ − propene, ▲ − acetylene, □ −ethylene, ◆ − ethane, △ − methane. The temperature dependent fits to a power law form are shown as solid lines.

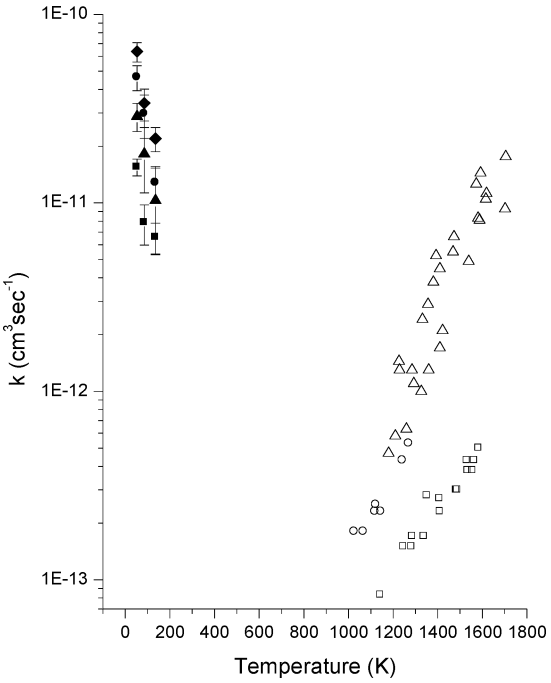

Figure 8. Temperature dependence of NH + unsaturated hydrocarbons. Filled symbols from this work: ◆ − diacetylene, ● − propene, ▲ − acetylene, ■ − ethylene. Open symbols from Rohrig et al.[11,12] using a shock tube appartus. ○ − propene, △ − acetylene, □ − ethylene.

energy surface without a barrier and are ideal candidates for study with the Laval technique, as their inverse temperature dependence onset usually occurs around 200 K. Further, it is interesting to note that uncertainty in the branching ratio for two thermodynamically accessible product channels exists. While Lee et al. have had success at determining the products for the reaction of C_2H radicals with acetylene[33] and O_2[34] using

the Laval method, it is by far not universal, and thus presents an interesting challenge to researchers in the field. The two thermodynamically accessible channels are

$$\mathrm{NH} + \mathrm{NO} \rightarrow \text{products} \quad \text{(R1)}$$

$$\mathrm{NH} + \mathrm{NO} \rightarrow \mathrm{N_2O} + \mathrm{H} \quad \Delta H_{\mathrm{rxn}} = -146\ \mathrm{kJ/mol} \quad \text{(R1a)}$$

$$\mathrm{NH} + \mathrm{NO} \rightarrow \mathrm{N_2} + \mathrm{OH} \quad \Delta H_{\mathrm{rxn}} = -407\ \mathrm{kJ/mol} \quad \text{(R1b)}$$

and both produce species that are potentially traceable in the flow. OH is easily monitored using LIF, while H atoms can be monitored through the chemiluminescent reaction with NO. The reaction is known to produce the HNO* intermediate, which decays by light emission to the red of 600 nm.[35] Harrison et al. failed to see either product species in their experiment, but argued that their OH detection scheme was far from optimal and are in favor of channel R1b. Yamasaki et al., using a room temperature fluorescence cell with appropriate laser systems for LIF detection of NH and OH, were able to measure both channel R1 and R1b independently and conclude that R1b accounts for nearly 100% of the branching.[9] These authors argue the sensibility of their results based on symmetry correlations between the HNNO intermediate $^2A''$ and the OH + N_2 products channel. However, Durant measured a branching fraction of 0.8 ± 0.4 for channel R1a and supported the result with theoretical calculations implicating the dissociation of the cis-HNNO isomer on the $^2A'$ surface as the responsible species for preferential branching to R1a due to a lower transition state energy.[5] Attempts were made in this study to monitor both of these product species; however, complications with both radicals, due to low count rates and high background fluorescence, precluded extraction of information regarding their concentration and thus branching ratio for R1.

While most of the interest in R1 has been generated at higher temperature due to its importance to combustion reactions, the low temperature behavior is nonetheless equally as interesting, as it appears that the reaction mechanism remains the same throughout the entire temperature range investigated. Further, observation of the inverse temperature dependence, with an onset near 150 K, provides information on the behavior of radical−radical reactions occurring at low temperature. While this reaction in particular is not implicated as being responsible for chemistry in chemically interesting environments such as Titan or the ISM, information on this sort is crucial for accurately modeling such situations, especially when considering the difficulty in experimentally obtaining accurate rate date for open shell systems.

The JPL recommendation for reaction R1 is $k_{298} = 4.9 \times 10^{-11}$ cm^3 s^{-1} with a barrier $E_a/R = 0 \pm 300$ K.[36] We suggest a global fit to the modified power law form, between 50 and 400 K, of $k(T) = (4.11 \pm 0.31) \times 10^{-11} \times (T/300)^{(0.30\pm0.17)} \times \exp^{((77\pm21)/T)}$ cm^3 s^{-1}. This fit is not anticipated to model the temperature dependence outside of this range. Physical interpretation of the parameters n and E_a is somewhat ambiguous, however fits to a power law form $A(T/300)^{-n}$, were found to poorly represent both data sets. The $A(T/300)^{-n}$ fit to just the low-temperature data produces $n = 0.54 \pm 0.11$.

The final motivation for conducting experiments on the NH + NO system was to serve as a calibrant for our measurement technique. Previous measurements with OH + HBr were found to be in accord with the available literature;[26] however, an independent validation was deemed desirable for the NH system especially when incorporating the new 53 K nozzle employing Ar buffer. As can be seen in Figure 6 the agreement of our data with the available measurements at higher temperature is quite good, and gives us confidence in the results.

4b. NH + Unsaturated Hydrocarbon Kinetics. The reactions of NH radical with unsaturated hydrocarbons, as illustrated in Figure 7, are also seen to manifest inverse temperature dependence over the temperature range explored. The $A(T/300)^{-n}$, best fit parameters reveal a few interesting details. First the temperature dependence for all reaction species, ethylene, acetylene, propene, and diacetylene are the same, within experimental error, and range in value from $n = (1.07 \rightarrow 1.23)$. This is not necessarily anticipated from a simple collision theory model for particles that attract with an $-aR^{-s}$ dependence. Under these circumstances the collision theory predicts a $T^{1/6}$ temperature dependence for the interaction of a dipole−induced dipole system, and a $T^{-1/6}$ dependence for a dipole−dipole interaction,[37] neither of which are observed. The independence of n on reaction partner, dipole−induced dipole for ethylene, acetylene, and diacetylene and dipole−dipole for propene, and also its nominal value of 1.1 for all systems, indicate that the dynamics of these systems is not described by simple classical capture theory. In addition, our calculation of k (50K) based on this model with an R^{-6} interaction potential predict a rate in the range of 2×10^{-10} cm^3/s, for the species in this investigation, nearly a factor of 3 higher than observed for the most reactive partner. However, it is not clear whether this analysis indicates that the reaction is occurring at approximately one-third of the collision frequency, or whether the model does not accurately represent the real potential. Indeed, it has been documented that long range capture theory is not as easily applied to neutral systems as it is to ion−molecule reactions and that detailed ab initio calculations on the PES are necessary.[38] Most probably the negative temperature dependence observed for the NH radical reactions with the unsaturated hydrocarbons is due to the lowering of the reagent rotational distribution as the temperature is decreased. This seems to be the most favored explanation and has been applied to the understanding of a number of chemical systems at low temperatures.[24]

4c. NH + Unsaturated Hydrocabon Mechanisms. Insights into the reaction mechanism and products formed can be gained by examining the thermochemistry and the trends in reactivity with regards to reactant complexity. NH radicals can potentially participate in either abstraction or addition chemistry; the addition channel involving either addition into a C−C or C−H bond. Abstraction of an H atom from the C−H bond of the hydrocarbons methane, ethane, and ethylene is endothermic, $\Delta H_{\mathrm{rxn}}(298\ \mathrm{K}) = 8.2$, 3.4, and 14.1 kcal/mol, respectively, and is thus not likely to be occurring in the low-temperature environment of the post nozzle flow. The heats of reaction were calculated using the $\Delta H_f(298\ \mathrm{K})$ values taken from Lias et al. and Chase.[39,40] Further, significant barriers are found in these cases at high temperature.[10] In contrast, the thermodynamics of the products formed from an NH addition into the π bond followed by stabilization, subsequent rearrangement, elimination, or bond cleavage is generally exothermic for the species ethylene, acetylene, propene, and diacetylene. The slow rates for NH + methane and ethane at 53 K, where only the abstraction channel is available, indicate that the endothermic hydrogen atom abstraction channel is not occurring at an appreciable rate under the conditions of our experiment. The methane rate is too slow to be measured using the current Laval technique, and $(1.1 \pm 4.3) \times 10^{-12}$ cm^3/s represents an upper bound to the actual rate. Contrary to the saturated hydrocarbons, fast reactivity is observed at all temperatures investigated for the unsaturated species, with the rate increasing with carbon

chain length, indicating that the addition mechanism is responsible. Attempts were made to correlate this effect to the ionization potential of the unsaturated species, as the low ionization potential of the unsaturated hydrocarbons has been implicated in facilitating addition reactions involving radical species,[41,42] as well as its cross section calculated from a simple geometric model, but correlations were not easily recognized.

Justification for an addition mechanism at low temperature can be gained by examination of other radical plus unsaturated species systems studied under similar conditions. Sims et al. have studied the reactions of CN($X^2\Pi$) with unsaturated hydrocarbons and speculate that the dominant mechanism is the addition of the radical to the π bond of the unsaturated hydrocarbon, leading to an exothermic displacement of an H atom by the CN group.[22] Canosa et al. also speculate that additions of CH radical to unsaturated hydrocarbons proceeds by a similar mechanism, in which a complex intermediate is formed and then dissociates producing a radical hydrocarbon and H atom. Further, they comment that the process is driven at low temperature by the high electron affinity of the radical and low ionization energy of the hydrocarbon species.[43] Clary et al., in a joint theoretical and experimental paper, pay extensive attention to the reaction of C(^3P_J) with acetylene.[44] The results from low-temperature experimental studies in the CRESU, crossed molecular beam experiments of integral and differential cross sections, and electronic structure and wave packet calculations show that the mechanism for this reaction proceeds through an initial addition complex of the C atom to the acetylinic bond. The addition complex can then access either of two product channels forming either $C_3H + H$ or the spin forbidden $C_3 + H_2$ products. In addition Leone and co workers in a series of studies have investigated the low-temperature reactivity of C_2H radical with unsaturated hydrocarbons, and come to the same conclusion that the mechanism involves an addition intermediate on an attractive potential energy surface, that leads to elimination of a H atom.[45−47]

More recently quantum chemical calculations have provided for a rigorous understanding of experimental kinetic data obtained using a crossed molecular beam apparatus for the systems $C_2(X\ ^1\Sigma_g^+, a\ ^3\Pi_u) + C_2H_4$,[48] $C_2(X\ ^1\Sigma_g^+, a\ ^3\Pi_u) + C_2H_2$,[49] and $C_2(X\ ^1\Sigma_g^+)$ and $C_3(X\ ^1\Sigma_g^+) + C_2H_4$.[50] These studies highlight the effect of the electronic potential on the reaction intermediates and outcome and allowed for the extraction of the reaction micro mechanism at the molecular level. Similar support for the NH + unsaturated hydrocarbon reactions would certainly be insightful.

Fueno et al. have performed ab initio CI calculations, employing the 4-31G basis set, on the NH($X\ ^3\Sigma^-$) + ethylene reaction and find considerable barriers (in excess of 10 kcal/mol) for the initial addition step to make the triplet diradical, as well as large barriers onto products.[51,52] Their main focus was the isomerizations on the singlet and triplet surfaces leading to the elimination product $CH_3CHN + H$. They estimate the error in their CI calculations to be about 2.4 kcal/mol, but these results appear inconsistent with the findings of these experiments, and most likely illustrate the inherent difficulty of calculating open shell energetics and geometries necessary to accurately represent reactive systems.

A combination of the behavior of similar radical/unsaturated systems at low temperature, in conjunction with the arguments presented based on thermodynamics and the reactivity observed leads us to believe that the mechanism for the reactions involving NH radical and unsaturated hydrocarbons involves the initial formation of an addition complex, via NH addition to the π bond. However, it is unclear whether the complex then decays via a number of thermodynamically accessible channels, which may involve H atom elimination, H_2 elimination (even though it is spin forbidden), or a C−C bond fission to produce a number of products, including nitriles, HCN, and/or free amines, or whether the addition complex is stabilized by a third body forming a triplet diradical adduct. The ratio of these channels would depend on a number of factors including the pressure, temperature, reaction thermochemistry, and the placement and height of barriers along the reaction potential energy surface.

Figure 8 combines the results of this work with previous studies conducted by Rohrig and Wagner[11] and Rohrig et al.[12] on the same systems at high-temperature behind incident shock waves. They find their data best represented by Arrhenius expressions, and the data are as follows: $k = (3.0 \pm 0.7) \times 10^{-12} \exp^{(-(6735\pm481)\mathrm{K}/T)}$ cm^3 s^{-1}, $k = (5.5 \pm 0.2) \times 10^{-11} \exp^{(-(6013\pm481)\mathrm{K}/T)}$ cm^3 s^{-1}, $k = (8.3 \pm 6.1) \times 10^{-10} \exp^{(-(7096\pm1082)\mathrm{K}/T)}$ cm^3 s^{-1}, for ethylene, propene, and acetylene, respectively. A question naturally arises regarding the factors that lead to the non-Arrhenius behavior observed. Normally, curvature in Arrhenius plots can be understood in terms of a change in the reaction mechanism. Mechanistically, Rohrig and Wagner argue for an addition/elimination process, but are unable to rule out contributions from the H atom abstraction channel, due to the limited temperature range of their study and their rate extraction method. They indicate that the contribution from abstraction could be as high as 50% for propene. If their measurements are of the more direct H atom abstraction process, the change in mechanism from addition at low temperature, to abstraction at high temperature is easy to envision. However, if indeed their laboratory measurements are of an addition/elimination process occurring with a barrier, their studies suggest that the low-temperature mechanism might involve a different portion of the potential energy surface accessing products without a barrier or a process resulting in the stabilization of the adduct formed from the initial collision.

Adduct formation is known to play an important role in the chemistry of hydroxyl radicals with hydrocarbon species and is perhaps useful for comparison to the NH + unsaturated hydrocarbon systems. The OH reactions have been extensively studied for their role in atmospheric chemistry over a wide range of pressure and temperature, and are reviewed by Atkinson.[53] Investigations of the pressure and temperature dependence of the rate coefficient reveal a falloff behavior and a negative temperature dependence of the rates for OH reactions with unsaturated hydrocarbons. The temperature and pressure dependent mechanism for these reactions is commonly understood in terms of a process involving the initial formation of a complex, which can either back dissociate to reactants, proceed to products, or stabilize the OH−alkene radical adduct through third body collisions. It is generally found that the adduct formation process occurs without an activation energy and the negative temperature dependence is associated with the preexponential factor. Specifically, for the case of OH + ethylene at room temperature the adduct formation is the dominant channel since the energy for production of vinyl alcohol ($HOCH{=}CH_2$) + H is approximately 7 kcal/mol endothermic with respect to reactants. Raising the temperature in these studies increases the importance of the thermal decomposition of the adduct and thus reduces the reaction rate. However, at higher temperatures the H atom abstraction pathway becomes accessible and Arrhenius behavior is observed with positive activation energy. The above OH chemistry is described to highlight the apparent similarities

with the data presented in Figure 8, where at low temperature the reaction is likely proceeding via a complex addition intermediate that can either be stabilized by collisions, or react in an elimination or fragmentation process. Under these circumstances, the data of Rohrig et al. is best understood as participation of NH in either addition/elimination or abstraction chemistry over a portion of the potential energy surface with a barrier. Moreover, the reactions of hydroxyl radical with propene ($k_{103K} = (0.81 \pm 0.18) \times 10^{-10}$ cm^3/s) and 1-butene ($k_{103K} = (1.24 \pm 0.27) \times 10^{-10}$ cm^3/s)[54] and with butenes ($k_{75K} \approx 3 \times 10^{-10}$ cm^3/s)[55] have been studied at low temperature in Laval nozzle expansions and their rates are found to be fast and display negative temperature dependence. Sims et al. find strong evidence for the absence of any maximum of electronic potential energy along the minimum energy path leading from separated reagents to the radical adduct for the OH + butanes reactions,[55] while Vakhtin et al. expect the reactions of OH + propene and 1-butene to be in their high-pressure limit under the low temperature and pressure conditions of their experiment.[54,56] More recently Vakhtin et al. have observed U-shaped Arrhenius plots for the reaction of OH with hydrogen peroxide at low temperature and attribute the behavior to a change in mechanism from abstraction at high temperature to formation of an intermediate complex at low temperature.[57]

With this in mind it seems reasonable to anticipate that the two hydride radicals will behave in a similar manner at low temperature and pressure. The measured rate for NH + propene at 83 K is $(2.97 \pm 0.77) \times 10^{-11}$ cm^3/s, approximately a factor of 2 smaller than the OH + propene system at similar temperature and flow conditions measured by Vakhtin et al.[54] Many possibilities could account for the slower reactivity of NH including the difference in dipole moment of the two diatomic radicals, the electron affinity, the electronic surface over which the reaction takes place, the stability of the radical adduct, and the number of product channels accessible.

Finally, Rohrig and Wagner[11] compare their data to the O(^{3}P) + hydrocarbon systems. They find good correlation between the barriers for the NH and O isoelectronic species with homologous reaction partners, and argue that this good correlation is a hint that the chemistries are the same, i.e., both are participating in electrophilic addition. While both O(^{3}P) and NH($^3\Sigma^-$) are isoelectronic, and both form a diradical upon addition, there is most probably a difference in the adduct formation mechanism. It is speculated that the imidogen dipole moment, just like that of hydroxyl, allows for the initial formation of an adduct on an attractive potential, while the O(^{3}P) experiences some electronic repulsion upon approach to the π system of the unsaturated species leading to a barrier. For the O(^{3}P) + unsaturated hydrocarbon systems barriers are common.[58]

5. Conclusion

The reactions of NH(X $^3\Sigma^-$) with NO and the hydrocarbons methane, ethane, ethylene, acetylene, propene, and diacetylene have been measure in a pulsed supersonic Laval nozzle flow reactor between 53 → 188 K. The reactions of NH with NO and the unsaturated hydrocarbons show inverse temperature dependence in the temperature range investigated, and best fits to the data sets have been suggested. For NH + NO good agreement of the data with that available in the literature was observed. The chemistry of the NH + unsaturated hydrocarbon systems is currently understood to occur at low temperature through an addition mechanism, but it is unclear at this time whether the adduct proceeds to products or is stabilized by additional collisions. Further, experiments focusing on the pressure dependence and kinetic isotope effects would help to resolve this issue, as would an accurate potential energy surface. An understanding of the chemistry of these systems will help to determine their importance to the atmospheric chemistry of Saturn's moon Titan, as well as other low-temperature environments where these molecules might be found.

Acknowledgment. The authors gratefully acknowledge financial support of this work by the National Science Foundation through Grant No. CHE-9984613. In addition C.M. would like to thank Dr. Andrey E. Belikov for his insight and scientific advice throughout the course of the experiments.

References and Notes

(1) Mertens, J. D.; Chang, A. Y.; Hansen, K.; Bowman, C. T. *Int. J. Chem. Kinet.* **1991**, *23*, 173.
(2) Yokoyama, K.; Sakane, Y.; Fueno, T. *Bull. Chem. Soc. Jpn.* **1991**, *64*, 1738.
(3) Vandooren, J.; Sarkisov, O. M.; Balakhnin, V. P.; Van Tiggelen, P. J. *Chem. Phys. Lett.* **1991**, *184*, 294.
(4) Sausa, R. C.; Anderson, W. R.; Dayton, D. C.; Faust, C. M.; Howard, S. L. *Combust. Flame* **1993**, *94*, 407.
(5) Durant, J. L. J. *J. Phys. Chem.* **1994**, *98*, 518.
(6) Harrison, J. A.; Whyte, A. R.; Phillips, L. F. *Chem. Phys. Lett.* **1986**, *129*, 346.
(7) Hansen, I.; Hoinghaus, K.; Zetzsch, C.; Stuhl, F. *Chem. Phys. Lett.* **1976**, *42*, 370.
(8) Cox, J. W.; Nelson, H. H.; McDonald, J. R. *Chem. Phys.* **1985**, *96*, 175.
(9) Yamasaki, K.; Okada, S.; Koshi, M.; Matsui, H. *J. Chem. Phys.* **1991**, *95*, 5087.
(10) Rohrig, M.; Wagner, H. G. *Ber. Bunsen-Ges. Phys. Chem.* **1994**, *98*, 858.
(11) Rohrig, M.; Wagner, H. G. *Ber. Bunsen-Ges. Phys. Chem.* **1994**, *98*, 864.
(12) Rohrig, M.; Romming, H. J.; Wagner, H. G. *Ber. Bunsen-Ges. Phys. Chem.* **1995**, *99*, 105.
(13) Mertens, J. D.; Chang, A. Y.; Hansen, K.; Bowman, C. T. *Int. J. Chem. Kinet.* **1989**, *21*, 1049.
(14) Baulch, D. L.; Cobos, C. J.; Cox, R. A.; Esser, C.; Frank, P.; Just, T.; Kerr, J. A.; Pilling, M. J.; Troe, J.; Walker, R. W.; Warantz, J. *J. Phys. Chem. Ref. Data* **1992**, *21*, 411.
(15) Baulch, D. L.; Cobos, C. J.; Cox, R. A.; Frank, P.; Hayman, G.; Just, T.; Kerr, J. A.; Murrells, T.; Pilling, M. J.; Troe, J.; Walker, R. W.; Warantz, J. *J. Chem. Phys. Ref. Data* **1994**, *23*, 847.
(16) Lillich, H.; Schuck, A.; Volpp, H.-R.; Wolfrum, J. *Symp. (Int.) Combust., [Proc.]* **1994**, *25*, 993.
(17) Romming, H. J.; Wagner, H. G. *Symp. (Int.) Combust., [Proc.]* **1996**, *26*, 559.
(18) Lara, L. M.; Lellouch, E.; Lopez-Moreno, J. J.; Rodrigo, R. *J. Geophys. Res., [Planets]* **1996**, *101*, 23261.
(19) Alagia, M.; Balucani, N.; Cartechini, L.; Casavecchia, P.; Volpi, G. G.; Pederson, L. A.; Schatz, G. C.; Lendvay, G.; Harding, L. B.; Hollebeek, T.; Ho, T. S.; Rabitz, H. *J. Chem. Phys.* **1999**, *110*, 8857.
(20) Casavecchia, P.; Balucani, N.; Alagia, M.; Cartechini, L.; Volpi, G. G. *Acc. Chem. Res.* **1999**, *32*, 503.
(21) Balucani, N.; Alagia, M.; Cartechini, L.; Casavecchia, P.; Volpi, G. G.; Sato, K.; Takayanagi, T.; Kurosaki, Y. *J. Am. Chem. Soc.* **2000**, *122*, 4443.
(22) Sims, I. R.; Queffelec, J.-L.; Travers, D.; Rowe, B. R.; Herbert, L. B.; Karthaeuser, J.; Smith, I. W. M. *Chem. Phys. Lett.* **1993**, *211*, 461.
(23) Carty, D.; Le Page, V.; Sims, I. R.; Smith, I. W. M. *Chem. Phys. Lett.* **2001**, *344*, 310.
(24) Smith, I. W. M.; Rowe, B. R. *Acc. Chem. Res.* **2000**, *33*, 261.
(25) Atkinson, D. B.; Smith, M. A. *Rev. Sci. Instrum.* **1995**, *66*, 4434.
(26) Atkinson, D. B.; Jaramillo, V. I.; Smith, M. A. *J. Phys. Chem. A* **1997**, *101*, 3356.
(27) Crosley, D. R.; Anderson, W. R. *Laser Excitation of Fluorescence in the A−X System of NH*; Technical Report ARBRL-TR-02260; Ballistics Research Laboratory, U. S. Army Armament Research and Development Command, Aberdeen Proving Ground: Aberdeen, MD; 1980.
(28) Brazier, C. R.; Ram, R. S.; Bernath, P. F. *J. Mol. Spectrosc.* **1986**, *120*, 381.
(29) Dixon, R. N. *Can. J. Phys.* **1959**, *37*, 1171.

(30) Smith, W. H.; Liszt, H. S. *J. Quant. Spectrosc. Radiat. Transfer* **1971**, *11*, 45.
(31) Armitage, J. B.; Jones, E. R. H.; Whiting, M. C. *J. Chem. Soc.* **1951**, *210*, 44.
(32) Lucht, R. P.; Peterson, R. C.; Laurendeau, N. M. *Fundamentals of Absorption Spectroscopy for Selected Diatomic Flame Radicals*; PURDU-CL-78−06; School of Mechanical Engineering, Purdue University: West Lafayette, IN, 1978.
(33) Lee, S.; Hoobler, R. J.; Leone, S. R. *Rev. Sci. Instrum.* **2000**, *71*, 1816.
(34) Lee, S.; Leone, S. R. *Chem. Phys. Lett.* **2000**, *329*, 443.
(35) Setser, D. W. *Reactive Intermediates in the Gas Phase: Generation and Monitoring*; Academic Press: New York, 1979.
(36) DeMore, W. B.; Sander, S. P.; Golden, D. M.; Hampson, R. F.; Kurylo, M. J.; Howard, C. J.; Ravishankara, A. R.; Kolb, C. E.; Molina, M. J. *Chemical Kinetics and Photochemical Data for Use in Stratospheric Modeling*; Evaluation Number 12, NASA, JPL, California Institute of Technology: Pasadena, CA, 1997.
(37) Johnston, H. S. *Gas-Phase Reaction Rate Theory*; The Ronald Press Company: New York, 1966.
(38) Liao, Q.; Herbst, E. *Astrophys. J.* **1995**, *444*, 694.
(39) Lias, S. G.; Bartmess, J. E.; Liebman, J. F.; Holmes, J. L.; Levin, R. D.; Mallard, W. G. *J. Phys. Chem. Ref. Data* **1988**, *17*.
(40) Chase, W. M. *J. Phys. Chem. Ref. Data; Monogr. 9* **1998**, *9*.
(41) Chastaing, D.; James, P. L.; Sims, I. R.; Smith, I. W. M. *Faraday Discuss.* **1998**, *109*, 165.
(42) Martinez, B.; Cabanas, A.; Aranda, J.; Albaladejo, R. P.; Wayne, J. *J. Chem. Soc., Faraday Trans.* **1997**, *93*, 2043.
(43) Canosa, A.; Sims, I. R.; Travers, D.; Smith, I. W. M.; Rowe, B. R. *Astron. Astrophys.* **1997**, *323*, 644.
(44) Clary, D. C.; Buonomo, E.; Sims, I. R.; Smith, I. W. M.; Geppert, W. D.; Naulin, C.; Costes, M.; Cartechini, L.; Casavecchia, P. *J. Phys. Chem. A* **2002**, *106*, 5541.
(45) Vakhtin, A. B.; Heard, D. E.; Smith, I. W. M.; Leone, S. R. *Chem. Phys. Lett.* **2001**, *348*, 21.
(46) Vakhtin, A. B.; Heard, D. E.; Smith, I. W. M.; Leone, S. R. *Chem. Phys. Lett.* **2001**, *344*, 317.
(47) Lee, S.; Samuels, D. A.; Hoobler, R. J.; Leone, S. R. *J. Geophys. Res., [Planets]* **2000**, *105*, 15085.
(48) Balucani, N.; Mebel, A. M.; Lee, Y. T.; Kaiser, R. I. *J. Phys. Chem. A* **2001**, *105*, 9813.
(49) Kaiser, R. I.; Balucani, N.; Charkin, D. O.; Mebel, A. M. *Chem. Phys. Lett.* **2003**, *382*, 112.
(50) Kaiser, R. I.; Le, T. N.; Nguyen, T. L.; Mebel, A. M.; Balucani, N.; Lee, Y. T.; Stahl, F.; Schleyer, P. v. R.; Schaefer, H. F. I. *Faraday Discuss.* **2001**, *119*.
(51) Fueno, T.; Bonacickoutecky, V.; Koutecky, J. *J. Am. Chem. Soc.* **1983**, *105*, 5547.
(52) Fueno, T.; Yamaguchi, K.; Kondo, O. *Bull. Chem. Soc. Jpn.* **1990**, *63*, 901.
(53) Atkinson, R. *Chem. Rev.* **1985**, *85*, 69.
(54) Vakhtin, A. B.; Lee, S.; Heard, D. E.; Smith, I. W. M.; Leone, S. R. *J. Phys. Chem. A* **2001**, *105*, 7889.
(55) Sims, I. R.; Smith, W. M.; Bocherel, P.; Defrance, A.; Travers, D.; Rowe, N. R. *J. Chem. Soc., Faraday Trans.* **1994**, *90*, 1473.
(56) Vakhtin, A. B.; Murphy, J. E.; Leone, S. R. *J. Phys. Chem. A* **2003**, *107*, 10055.
(57) Vakhtin, A. B.; McCabe, D. C.; Ravishankara, A. R.; Leone, S. R. *J. Phys. Chem. A* **2003**, *107*, 10642.
(58) Huie, R. E.; Herron, J. T. *Prog. React. Kinet.* **1975**, *8*, 1.